1493 (1979); *Tetrahedron*, **37**, 1359 (1981); (c) M. C. Pirrung, *J. Am. Chem. Soc.*, **101**, 7130 (1979); *ibid.*, **103**, 82 (1981); (d) W. G. Dauben and D. M. Walker, *J. Org. Chem.*, **46**, 1103 (1981); (e) P. A. Wender and G. B. Dreyer, *Tetrahedron*, **37**, 4445 (1981); (f) E. Wenkert and T. S. Arrhenius, *J. Am. Chem. Soc.*, **105**, 2030 (1983); (g) B. C. Ranu, M. Kavka, L. A. Higgs, and T. Hudlicky, *Tetrahedron Lett.*, **25**, 2447 (1984); (h) Y. Tobe, T. Yamashita, K. Kakiuchi, and Y. Odaira, *J. Chem. Soc., Chem. Commun.*, 898 (1985); (i) G. G. G. Manzardo, M. Karpf, and A. S. Dreiding, *Helv. Chim. Acta*, **69**, 659 (1986).
4. H. W. Lee and I.-Y. C. Lee, *Bull. Korean Chem. Soc.*, **11**, 273 (1990).
5. (a) G. Stork, *Pure Appl. Chem.*, **9**, 131 (1964); (b) R. E. Ireland, P. A. Aristoff, and C. F. Hoyng, *J. Org. Chem.*, **44**, 4318 (1979).
6. S. Danishefsky, R. Zamboli, M. Kahn, and S. J. Etheredge, *J. Am. Chem. Soc.*, **102**, 2097 (1980).
7. S. C. Welch and S. Chayabunjonglerd, *J. Am. Chem. Soc.*, **101**, 6768 (1979).
8. A. Leon-Bay and L. A. Paquette, *J. Org. Chem.*, **46**, 4173 (1982).
9. B. M. Trost and D. P. Curran, *J. Am. Chem. Soc.*, **103**, 7380 (1981).
10 G. Geetha, N. Raju, K. Rajagopalan, and S. Swaminathan, *Ind. J. Chem.*, **B20**, 238 (1981).
11 J. C. Stowell, *J. Org. Chem.*, **41**, 560 (1976).
12 G. Bauduin and Y. Pietrasanta, *Tetrahedron*, 4225 (1973).
13 T. Tsunoda, M. Suzuki, and R. Noyori, *Tetrahedron Lett.*, 1357 (1980).

Effects of van der Waals Bonding on the Collisional Dissociation of a Highly Excited Chemical Bond

Yoo Hang Kim and Hyung Kyu Shin†

Department of Chemistry, Inha University, Inchon 402-751
†Department of Chemistry, University of Nevada, Reno, Nevada 89557, USA. *Received March 12, 1991*

Dissociation of a highly excited diatomic molecule in the $Ar+Ar\cdots O_2$ and $Ar+O_2$ collisions is studied using trajectory dynamics procedures in the collision energy range of 0.050 to 1.0 eV. Between 0.050 and 0.2 eV, dissociation probabilities are very large for the complexed system compared to the uncomplexed system. This efficient dissociation of O_2 in $Ar\cdots O_2$ is attributed to the ready flow of energy from the incident atom to the large-amplitude vibrational motion of the excited O_2 *via* the van der Waals bond. Thermal-averaged dissociation probabilites of O_2 in $Ar+Ar\cdots O_2$ near room temperature are nearly two orders of magnitude larger than those of O_2 in $Ar+O_2$.

Introduction

In recent studies on the collision dynamics of van der Waals (vdW) complexes, we have shown that excitation of vdW complexes is very efficient and that the energy initially present in a high-frequency chemical bond remains when the collision is over.[1,2] When a heavy mass barrier is present between vdW bonds, energy flow from one vdW bond to another becomes seriously hindered and energy localizes in one of the weak bonds.[3,4] Energy flow blockage in molecular systems by heavy atoms or multiple bonds has been investigated by many researchers in recent years.[4-15] In a vdW complex involving diatomic and rare gas atom units, the chemical bond essentially conserves its individuality and experiences weak dynamical coupling with the vdW bond because of the large disparity in oscillator frequencies. Energy transfer to the chemical bond is, therefore, inefficient and the energy initially present in the bond remains when the collision is over. However, a new situation arises when the chemical bond is highly excited, especially to near the dissociation thereshold. At such excitation, the chemical bond becomes seriously weakened and undergoes a low-frequency vibrational motion, which may even be comparable to that of the vdW bond. In the complex with such a highly excited bond, a weak coupling between the vdW and chemical bonds can become sufficient to induce efficient intramolecular energy flow, thus causing the molecular unit to gain enough energy for dissociation.

The purpose of this paper is to study the effects of vdW bonding on the dissociation of O_2 in $Ar\cdots O_2$, in which the chemical bond is in a highly excited state. Such a complexed state is particularly important in the studies of thermal dissociation of O_2 dispersed in the argon gas or in the argon matrix.[16] In this model system, another Ar atom is incident on the complex to perturb its internal state. This collision-induced intramolecular dynamics will be treated in classical mechanics by sampling a sufficiently large number of trajectories in the collision energy range of 0.050 to 1.0 eV. The result will then be compared with that of $Ar+O_2$ to discuss the effects of vdW bonding on the dissociation of O_2 in the complex. In both the complexed and uncomplexed systems, O_2 is initially either in the ground state or in a highly excited state with the vibrational energy equal to 99% of the dissociation energy.

Interaction Model

For the incident Ar approaching the linear complex $Ar\cdots O_2$

from the left, we denote the relative separation by x. For convenience, we number the collision system Ar+Ar···O=O as 1+2···3=4. To describe the collision system, it is convenient to convert the kinetic energy expressed as $T=1/2\Sigma m_i(dx_i/dt)^2$, where $i=1\sim4$, into the center-of-mass coordinate expression

$$T=\tfrac{1}{2}\mu(dx/dt)^2+\tfrac{1}{2}M_L(dx_{23}/dt)^2\tfrac{1}{2}M_{O_2}(dx_{34}/dt)^2 \qquad (1)$$

where x_{23} is the displacement of the distance between Ar and the left-hand-side O in the complex from its equilibrium values d_{23}, x_{34} is the displacement of the O_2 bond distance from its equilibrium value d_{34}, μ is the reduced mass of the collision system, $M_L=m_2(m_3+m_4)/m$, $m=m_2+m_3+m_4$, and M_{O_2} is the reduced mass of O_2. In the complex, there is a large disparity in the vibrational frequencies of the oscillators. Because of this large disparity in oscillator frequencies, we expect the molecular unit O_2 to conserve its individuality and to experience weak dynamical coupling with the weak vdW bond in the complex, which can thus be considered to have two internal degrees of freedom. When the molecular unit is highly excited, its bond is weakened and undergoes a large amplitude vibration, whose frequency may now be comparable to that of the vdW bond. Therefore, even such a weak coupling can produce an efficient energy flow between the vdW and molecular bonds. The intramolecular potential energy of O_2 will be expressed in terms of a Morse function $V_{34}(x_{34})=D_{34}(1-e^{-x_{34}/b_{34}})^2$, where D_{34} and b_{34} are potential constants. The vdW interaction $V_{23}(x_{23})$ will be also specified by a Morse function. For this interaction, the potential well is very shallow (it is only 0.0111 eV as shown below) and the potential is highly anharmonic. For such a case, the Morse potential has been known to describe the interaction adequately. Beswick and Jortner have used this function in their detailed studies of the vibrational predissociation dynamics of diatomic dimers such as $H_2\cdots O_2$ and $CO\cdots N_2$.[17] In a recent study of the predissociation of $He\cdots I_2\cdots Ne$, where I_2 is vibrationally excited in the B $^3\Pi_{0u}^+$ electronic state, Villarreal *et al.* have used the Morse function for all interatomic interactions.[18] It is important to note that for Ar···HCl, differential elastic scattering cross section data fit the Morse function very well in the distance range of 0 to 4.453 Å.[19] When the potential function is parametrized in terms of the reliable well depth, equilibrium distance, and range parameter, the Morse potential is well suited for the study of intramolecular dynamics. Another function used to describe this type of intercation is the exp-6 potential, where the inverse 6th-power term represents the weak dispersion and induction effects.[20,21] In this potential, however, the 6th-power term tends to dominate the repulsive term at short range. To obtain realistic potential functions, therefore, complicated damping functions have to be introduced in such forms (*i.e.*, in the exp-6 or exp-6-8 form).[21] Although these potential functions describe better the intramolecular interaction of a vdW complex over a wider range of internal coordinates, they are difficult to formulate and use for the study of collision-induced intramolecular energy flow. Finally, the availability of still another function, the Lennard-Jones (12-6) potential[16] with additional long range terms, should by mentioned but the repulsive part of this inverse-power potential is much too steep for the soft vdW interaction.

Since the displacement x_L of the distance between Ar and the center-of-mass of O_2 in the complex from the equilibrium value d_L is related to the Ar···O distance $d_{23}+x_{23}$ as $d_L+x_L=d_{23}+x_{23}+\frac{1}{2}(d_{34}+x_{34})$, we can express the vdW interaction by $V_{23}(x_{23})=D_{23}(1-e^{-x_L/b_{23}+x_{O_2}/2b_{23}})^2$ where $x_{34}=x_{O_2}$. The exponential dependence of the potential function on x_L and x_{O_2} clearly represents the coupling of the two vibrational modes. Then the total interaction potential energy is

$$V=D_{23}(1-e^{-x_L/b_{23}+x_{O_2}/2b_{23}})^2+D_{34}(1-e^{-x_{O_2}/b_{34}})^2+V_I \qquad (2)$$

The last term represents the interaction of the incident Ar with the left-hand-side O atom of the complex, and it will be represented by $V_I=Ae^{-z/a}$, where z is the distance between the incident atom and the left-hand-side atom. Here A is a parameter that sets the classical turning point of the collision event and a sets the slope of the repulsive interaction potential wall. Since the role of this interaction is merely to perturb oscillator states and induce translation-to-vibration (TV) energy transfer in the present model, the use of such a simple function is sufficient here.[22] Note that for the Ar-Ar interaction the attractive energy is very weak, and it does not affect TV energy transfer significantly. On the other hand, if we were interested in studying the formation of complexes (*e.g.*, $Ar+Ar\cdots O_2\rightarrow Ar\cdots Ar\cdots O_2$), the attractive interaction between the incident atom and the complex is of major importance and a function such as the Morse interaction has to be used for V_I. Since the Ar-Ar distance is $z=x-[(m_3+m_4)/m](d_L+x_L)$, we find $V_I(x, x_L)=A'e^{-x/a+[(m_3+m_4)/m](x_L/a)}$, where $A'=Ae^{[(m_3+m_4/m](d_L/a)}$. Note that the intermolecular TV coupling is seen in $V_I(x, x_L)$. A complete study of collision-induced energy transfer and bond dissociation should be based on the use of a more realistic vdW potential obtained by fitting to the infrared and hyperfine spectra. Unfortunately, the existing data are not sufficient to determine such functions for the present system. Until such functions become available, however, we can use the above overall interaction potential V, which describes some of the essential features of the present collision system, such as the intra- and intermolecular mode coupling for the collinear configuration, as well as vibrational anharmonicity.

The equations of motion for the vdW bond, molecular unit O_2, and relative motion are

$$M_L(d^2x_L/dt^2)=-2(D_{23}/b_{23})f_L-[A(m_3+m_4)/am]f_x \qquad (3)$$

$$M_{O_2}(d^2x_{O_2}/dt^2)=-2(D_{34}/b_{34})f_{O_2}+(D_{23}/b_{23})f_L \qquad (4)$$

$$\mu(d^2x/dt^2)=(A/a)f_x \qquad (5)$$

where $f_L=(1-e^{-x_L/b_{23}+x_{O_2}/2b_{23}})e^{-x_L/b_{23}+x_{34}/2b_{23}}$, $f_{O_2}=(1-e^{-x_{O_2}/b_{34}})e^{-x_{O_2}/b_{34}}$, and $f_x=e^{-x/a+(m_3+m_4)x_L/ma}$. For $Ar+O_2$, $T=1/2\mu(dx/dt)^2+1/2M_{O_2}(dx_{O_2}/dt)^2$ and $V=D_{O_2}(1-e^{-x_{O_2}/b_{34}})^2+V_I$, where V_I is now simply $A'e^{-x/a+x_{O_2}/2a}$, where $A'=Ae^{d_{O_2}/2a}$. Note that in this case μ is the reduced mass of $Ar+O_2$ and x is the relative separation between Ar and O_2. Also note that a now represents the range parameter for the interaction between Ar and O_2 while that in the above case is for the interaction between two argon atoms. The equations of motion are $M_{O_2}(d^2x_{O_2}/dt^2)=-(\partial V/\partial x_{O_2})$ and $\mu(d^2x/dt^2)=-(\partial V/\partial x)$.

Computational Details

We solve the equations of motion using standard numerical routines[23] for the initial conditions x_L°, $x_{O_2}^\circ$ and x°. Initi-

ally, $x=\infty$ and $V_I=0$, *i.e.*, $f_x=0$. Therefore, the initial conditions are the solution of

$$M_L(d^2x_L/dt^2) = -2(D_{23}/b_{23})f_L \quad (6)$$

$$M_{O_2}(d^2x_{O_2}/dt^2) = -2(D_{34}/b_{34})f_{O_2}+(D_{23}/b_{34})f_{O_2} \quad (7)$$

evaluated at $t=t^\circ$. These solutions depend on the initial vibrational energies (E°_{v,O_2} and $E^\circ_{v,L}$) and initial vibrational phases of the bond O_2 and $L(\delta_{O_2}$ and $\delta_L)$; *i.e.*, $x_L^\circ \equiv x_L^\circ(t^\circ, \delta_L, E^\circ_{v,L})$ and $x_{O_2}^\circ \equiv x_{O_2}^\circ(t^\circ, \delta_{O_2}, E^\circ_{v,O_2})$. We take the O_2 unit to be in either the ground state($E^\circ_{v,O_2}=\frac{1}{2}\hbar\omega$) or a highly excited state(specifically $E^\circ_{v,O_2}=0.99D_{O_2}$), while $E^\circ_{v,L}=\frac{1}{2}\hbar\omega_L$, where ω_L is the vibrational frequency of the vdW bond. Here, t° is the initial value representing a large negative time (*i.e.*, before collision), so the time-dependent solutions of x_{O_2}, x_L, x and their derivatives are obtained by integrating the equations of motion from $t=t^\circ$ to a final time t.

To determine the initial conditions for the relative motion, we note that the interacion potential V_I reduces to $V_I^\circ = A'e^{-x/a}$ when x is sufficiently large such that $x \gg x_L$. The initial conditions are then obtained from the solution of the equation $\frac{1}{2}\mu(dx/dt)^2+V_I^\circ=E$, where E is the initial collision energy:

$$x(t^\circ) = -2a \ln\{\text{sech}[(E/2\mu)^{1/2}(t^\circ/a)]\} \quad (8)$$

$$p(t^\circ) = (2\mu E)^{1/2} \tanh[(E/2\mu)^{1/2}(t^\circ/a)] \quad (9)$$

In deriving these two equations, which apply to both Ar+Ar$\cdots O_2$ and Ar+O_2, we equated the intermolecular potential constant A' to E to set the energy scale. Therefore, the time-dependent solutions of the equations of motion are $x_L \equiv x_L(t, \delta_L, \delta_{O_2}, E^\circ_{v,L}, E^\circ_{v,O_2}, E)$ and $x_{O_2} \equiv x_{O_2}(t, \delta_L, \delta_{O_2}, E^\circ_{v,L}, E^\circ_{v,O_2}, E)$ where each of the phases is sampled randomly.

In solving the equations of motion, the number of intergration steps is adjusted so as to maintain the step size of about 1/20th of the O_2 vibration period. The initial relative separation $x(t^\circ)$ is fixed and must be great enough to ensure that the interaction is negligible; we take this value to be about 15 Å throughout the calculation. A trajectory is terminated when the final distance $x(t)$ is at least equal to the initial separation; *i.e.*, the collision is terminated when the time is sufficiently long such that $x(t)$ has receded far away from the collision region. Dissociation is assumed to have occurred when the bond displacement x_{O_2} exceeds 3.5 Å. However, the highly excited molecular unit in Ar$\cdots O_2$ often fails to dissociate even after reaching the value. In such a case, we confirm the occurrence of dissociation by following the trajectory for a sufficiently long time to ensure the receding atoms are not attracted back and checking the amount of energy transfer to O_2, which must exceed the critical energy needed for the molecule to dissociate. Furthermore, the momentum $p_{O_2}=M_{O_2}(dx_{O_2}/dt)$ levels off to a constant value as the dissociation occurs. At a given collision energy, the dissociation probability is defined as the ratio of the number of dissociative trajectories to the total number of trajectories randomly sampled.

Energy transfers to O_2 and the vdW bonds are, respectively, $\Delta E_{O_2}(t)=E_{O_2}(t)-E^\circ_{v,O_2}$ and $\Delta E_L(t)=E_L(t)-E^\circ_{v,L}$, where the vibrational energy associated with each bond is determined by adding the kinetic and potential energies; *e.g.*, $E_{O_2}(t)=\frac{1}{2}M_{O_2}(dx_{O_2}/dt)^2+D_{34}[1-e^{-x_{O_2}(t)/b_{34}}]^2$. In Ar+Ar$\cdots O_2$, the sum of these two energy transfers is the total amount of energy transfer to the complex. When the collision is over, the momentum of the relative motion $p=\mu(dx/dt)$ takes a constant value, so the energy tranfer levels off to the limiting ($t\rightarrow+\infty$) value $\Delta E(+\infty, \delta_L, \delta_{O_2}, E^\circ_{v,L}, E^\circ_{v,O_2}, E)$ while the vibrational energies of O_2 and the vdW bond still vary as a result of continuing intramolecular energy redistribution. This internal energy flow persists untill dissociation is completed. In the limit $t\rightarrow+\infty$, this sum is identical to $(2\mu)^{-1/2}[p(t^\circ)^2-p(+\infty)^2]$ for a particular phase set (δ_L, δ_{O_2}) with a given value of E. Here $p(t^\circ)$ and $p(+\infty)$ are the values of the momentum of the relative motion at the beginning and end of the trajectory; $p(+\infty)\equiv p(+\infty, \delta_L, \delta_{O_2}, E^\circ_{v,L}, E^\circ_{v,O_2}, E)$. The average of the phase-dependent energy transfer $\Delta E(+\infty, \delta_L, \delta_{O_2}, E^\circ_{v,L}, E^\circ_{v,O_2}, E)$ over phases δ_L and δ_{O_2} will be denoted simply by ΔE in the following section. The quantity $\Delta E(t)$ represents the phase-averaged energy transfer at time t. At a given collision energy, we sample at least 720 trajectories using standard Monte Carlo routine[24] of initial phases.

In the numerical integration of the equations of motion for the Ar+O_2 collision, we take $\omega_e=1580$ cm^{-1} for the fundamental frequency of the O_2 molecule and 5.080 eV for D_e.[25] The anharmonicity constants are $\omega_e x_e=12.0730$ cm^{-1} and $\omega_e y_e=0.0546$ cm^{-1}.[25] Note that the quantity ω used throughout this paper is the angular frequency and is related to the fundamental by $\omega=2\pi\omega_e$. The O_2 dissociation energy used in the calculation is then $D_{34}=D_{O_2}=D_e+\frac{1}{2}\hbar\omega=5.177$ eV. The intramolecular Morse potential constant $b_{34}=(2D_{34}/M_{O_2})^{1/2}(1/\omega)=0.375$ Å. The interaction range paramer a for Ar+O_2 is 0.256 Å.[26] To determine the range parameter a for the interaction of the incident atom with the left-hand-side of the complex in Ar+Ar$\cdots O_2$, we use the energy $D_{Ar\text{-}Ar}=91.6$ cm^{-1} and the frequecy $\omega_{Ar\text{-}Ar}=30.7$ cm^{-1}. Then, $a=(D_{Ar\text{-}Ar}/2M_{Ar\text{-}Ar})^{1/2}(1/\omega_{Ar\text{-}Ar})=0.286$ Å, where $M_{Ar\text{-}Ar}=m_{Ar}m_{Ar}/(m_{Ar}+m_{Ar})$. Note that Farrar and Lee used the same value of a for the Ar+HCl interaction potential, where HCl is isoelectronic to Ar.[19] From $D_{O_2\text{-}O_2}=87.0$ cm^{-1} and $D_{Ar\text{-}Ar}=91.6$ cm^{-1},[16,17] we determine $D_{23}=0.0111$ eV and $\omega_L=(2D_{23}/M_L)^{1/2}(1/b_{23})=35.9$ cm^{-1} for the Ar$\cdots O_2$ interaction, where $b_{23}=0.513$ Å. The frequency of O_2 in the Ar$\cdots O_2$ is 1556 cm^{-1}.[16]

Results and Discussion

Vibrational Energy Transfer. For O_2 in the ground state of uncomplexed system, the amount of phase-averaged energy transfer expressed in the fractional quantity $\Delta E/E$ is plotted in Figure 1. In the numerical procedures for this uncomplexed system, for example at $E=1.0$ eV, we start the integration at $t^\circ=-0.45$ ps; at this initial time, the incident atom is 14 Å away from the complex. The interaction begins near $t=-0.10$ ps, *i.e.*, 0.35 ps after t°, and the incident atom reaches its closest distance to the target at $t_c=0$ after which it bounces off to infinity. The collision is over near $t=+0.10$ ps at which the incident atom is 3.1 Å away from the target molecule. All trajectories at this collision energy are allowed to propagate until the final time of +0.66 ps has been reached. At this time, the incident Ar atom is 21 Å away from the target. The amount of energy transfer at $E=1.0$ eV is $\Delta E/E=2.3\times10^{-4}$. It should be noted that for O_2 in the ground state, when the model of harmonic oscillation is used, an explicit expression for the energy transfer

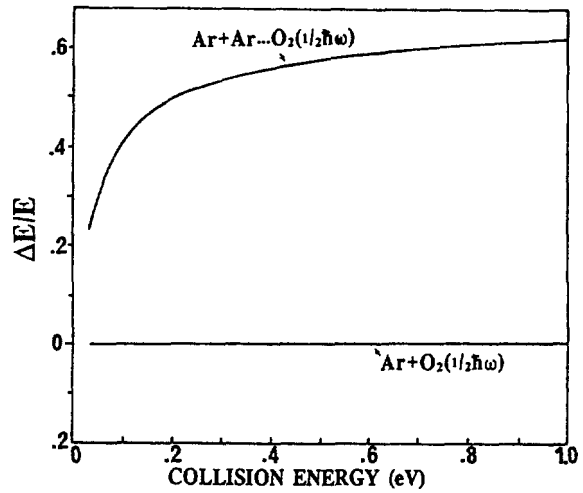

Figure 1. Dependence of the phase-averaged energy transfer to the complex $\Delta E/E$ on the collision energy E for Ar+Ar···O_2 ($\frac{1}{2}\hbar\omega$) and Ar+O_2 ($\frac{1}{2}\hbar\omega$).

for Ar+O_2 can be obtained in the form[28,29]

$$\Delta E/E=[(\pi\mu a\omega)^2/2M_{O_2}E]\,\mathrm{csch}^2[\pi a\omega(\mu/2E)^{1/2}] \quad (10)$$

This expression gives $\Delta E/E=2.2\times10^{-4}$ at $E=1.0$ eV. At lower collision energies, translation-to-vibration (TV) energy transfer $\Delta E/E$ in the collision between Ar and the uncomplexed O_2 molecule is much less than 10^{-4}.

When the molecule is complexed, energy transfer becomes very efficient; this situation is clearly seen in Figure 1. As shown in the Figure, energy transfer to the complex in Ar+Ar···O_2 ($\frac{1}{2}\hbar\omega$) increases from $\Delta E/E=0.41$ at $E=0.10$ eV to 0.62 at 1.0 eV. Such a large value is due to a preferential energy transfer to the weak bond which subsequently dissociates and excess energy is carried away by the fragments as the kinetic energy. As in the uncomplexed case, collisional energy transfer to the ground state O_2 unit itself in the complex is very small as a result of the inefficient TV energy flow between the translational motion and the vibrational motion of a high-frequency chemical bond. We also find that in the collision energy range from 0.05 to 1.0 eV, the vdW bond always dissociates. Since $D_L=0.0111$ eV, a trajectory representing an energy transfer efficiency greater than 22% at 0.05 eV can lead to the dissociation of this weak bond.

We now consider the case where the molecule is in a highly excited state. The excited molecular unit undergoes a large-amplitude vibrational motion and its frequency is far less than the fundamental. The excited molecule O_2 (0.99 D_{O_2}) vibrates with the frequency 157 cm^{-1}, which is about 1/10th the O_2 fundamental frequency 1580 cm^{-1}. At $E=0.1$ eV, O_2 is deexcited for $\delta_{O_2}=0$ and the frequency of the deexcited O_2 is 185 cm^{-1} (Note that if it is deexcited all the way to the ground state, the frequency would be 1580 cm^{-1}). For this representative trajectory of the nondissociative case, the power spectrum of the vibration of O_2 obtained from the expression[3]

$$I(\omega;\,E)=\left|\,(1/T)\int_{t^\circ}^{t^\circ+T}x_{O_2}(t,\,E)\exp(j\omega t)\,dt\,\right|^2 \quad (11)$$

shows this and overtone frequencies; see Figure 2a. In this

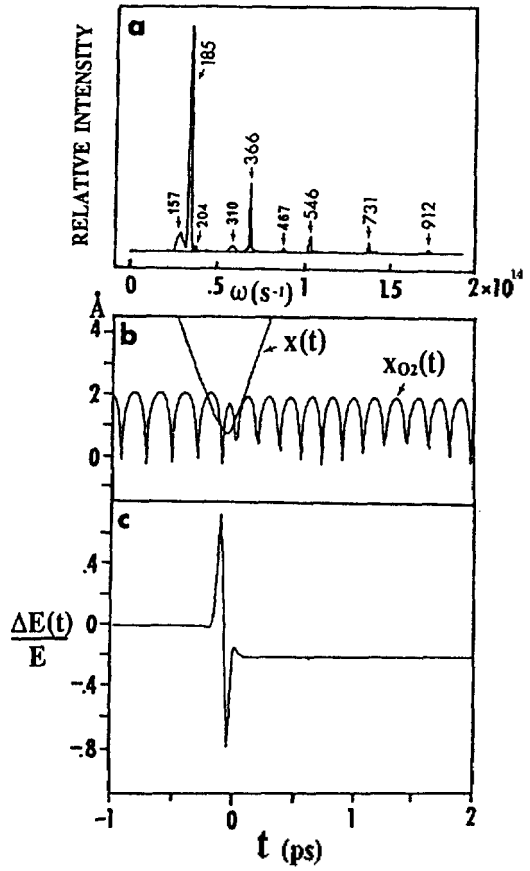

Figure 2. Ar+O_2 (0.99D_{O_2}) for $\delta_{O_2}=0°$ at $E=0.10$ eV. (a) power spectrum of O_2 vibration; numbers represent vibrational frequencies in cm^{-1}. (b) time-dependence of the vibration of O_2 and collision trajectory $x(t)$. (c) time evolution of phase-averaged energy transfer $\Delta E(t)/E$.

equation, the time length T of the data segment starting from t° is Fourier analyzed. For this particular trajectory, we integrated the equations of motion from $t^\circ=-1.40$ ps to $t=+5.50$ ps. Therefore, by taking $T=1.40+5.50=6.90$ ps, we can construct the spectrum of O_2 vibration over the entire time range of before, during, and after collision. Such a spectrum contains far more interesting features than the collision-free case (*e.g.*, before collision) since it contains contributions coming from all regions of the dynamical process. The major peak appears at $3.49\times10^{13}\,s^{-1}$ (185 cm^{-1}), which is blue-shifted from the collision-free frequency of 2.97×10^{13} s^{-1}(157 cm^{-1}). A low-intensity peak appearing at the left of the major peak stands for this collision-free case. Note that if O_2(0.99D_{O_2}) is excited without dissociation, its frequency would be red-shifted and that if it is deexcited all the way to the groud state, the frequency would be blue-shifted to 1580 cm^{-1}. The frequency of a tiny peak appearing slightly above the major peak is $3.84\times10^{13}\,s^{-1}$ or 204 cm^{-1} and it represents the O_2 vibration during collision. The appearance of overtone peaks with significant intensity indicates the importance of the oscillator anharmonicity of the excited O_2 molecule. The overtone peaks at 157, 310 and 467 cm^{-1} are for the vibration of O_2(0.99D_{O_2}) before collision, and those at 185, 366, 546, 731 and 912 cm^{-1} are for the vibration of O_2 after collision in Ar+O_2 (0.99D_{O_2}), where

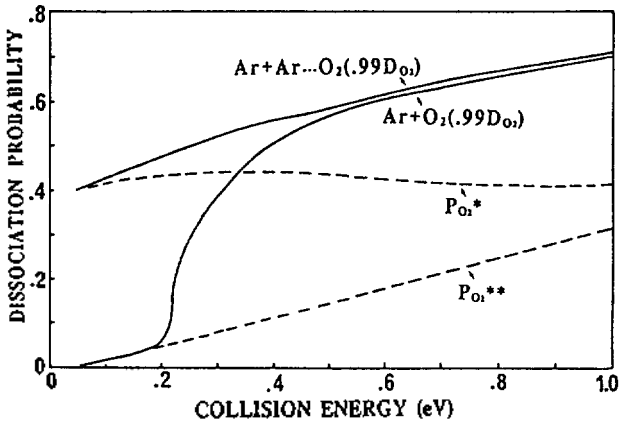

Figure 3. Dependence of the probability of O_2 dissociation, P_{O_2} on the collision energy E for $Ar+Ar\cdots O_2$ $(0.99D_{O_2})$ and $Ar+O_2$ $(0.99D_{O_2})$. Also shown are the pre-impact probability $P_{O_2}^*$ and the post-impact probability $P_{O_2}^{**}$.

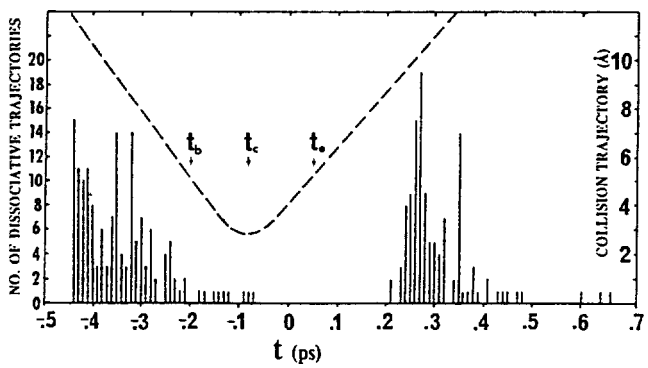

Figure 4. Distribution of dissociative trajectories in $Ar+Ar\cdots O_2$ $(0.99D_{O_2})$ at $E=1.0$ eV. Also shown is the collision trajectory $x(t)$; see the right-hand-side scale. The collision begins at t_b and ends at t_e; the collision partners reach the distance of closest approach at t_c.

the deactivation of O_2 $(0.99D_{O_2})$ has occurred. (Note that, for example, for the phase set $(\delta_L, \delta_{O_2})=(100°, 0°)$ representing the nondissociative trajectories of $Ar+Ar\cdots O_2$ $(0.99D_{O_2})$, the collision-free frequency is 167 cm^{-1} and is blue-shifted to 174 cm^{-1} after collision). To discuss these vibrational motions in the uncomplexed system further, we now consider the time dependence of O_2 vibration in the following paragraph.

In Figure 2b, we plot the vibration of O_2 in the uncomplexed collision system $Ar+O_2$ $(0.99D_{O_2})$ between $t=-1$ and $+2$ ps for $\delta_{O_2}=0°$ at $E=0.1$ eV; also shown is the collision trajectory $x(t)$ to indicate the distance of closest approach, which occurs near $t=0$. The calculation shows that the collision between Ar and O_2 begins at $t=-0.26$ ps and ends at $+0.12$ ps; *i.e.*, the duration of collision is 0.38 ps. Therefore, $x_{O_2}(t)$ plotted in the figure represents the entire range of collision, *i.e.*, before (-1 to -0.26 ps), during (-0.26 to $+0.12$ ps), and after ($+0.12$ to $+2.0$ ps) collision. The figure clearly shows the variation of vibrational period during the course of these dynamical processes. It is interesting to examine the time evolution of energy transfer $\Delta E(t)/E$ and collision tranjectory $x(t)$ of this nondissociative case. As shown in Figure 2c, at the initial impact with Ar, the vibrational energy transfer to O_2 rises to a value as high as $\Delta E/E=0.7$, but the receding Ar atom takes back all of this energy and some additional energy from the vibrational motion of O_2. Eventually, for this particular trajectory, the initially excited O_2 loses $\Delta E/E=0.2$ when the collision is over. We should mention that the peak height of 0.7 during the collision indicates that the molecule gains $\Delta E=0.07$ eV, which exceeds the minimum energy 0.0518 eV needed to dissociate, but the energy resides in the bond for a duration much shorter than the period of O_2 $(0.99D_{O_2})$ oscillation, which is 0.21 ps, so the bond cannot dissociate. The calculation shows that the width of the peak at half its maximum height is only 0.052 ps.

O_2 Bond Dissociation. The ground-state molecule O_2 does not dissociate in both $Ar+Ar\cdots O_2$ and $Ar+O_2$ in the collision energy considered. However, when O_2 is excited to have the initial vibrational energy $E_{v,O_2}^{\circ}=0.99$ D_{O_2} O_2 dissociation occurs in both collisions and we now study the effect of the vdW bond on this dissociation. The probability of O_2 dissociation in the $Ar+Ar\cdots O_2$ $(0.99D_{O_2})$ collision is very large; see Figure 3. The dissociation probability P_{O_2} is ~ 0.4 at $E=0.05$ eV and gradually increases to a value as large as 0.74 at $E=1.0$ eV. Since the vibrational frequency of the highly excited O_2 unit in the complex is very small, there is an efficient energy flow between the vdW bond and this seriously weakened molecular bond during the collision. This flow efficiently mediates energy transfer from the translational motion to the molecular unit and can eventually lead to the dissociation of both O_2 and vdW bonds. Although the molecule is highly excited, on the other hand, the excitation of O_2 through direct encounter with the incident argon atom in $Ar+O_2$ $(0.99D_{O_2})$ is not very efficient especially at low collision energies and this leads to dissociation probabilities which are significantly smaller than those of the complexed system; see the curve at collision energies below 0.2 eV in Figure 3. However, when the collision energy increases from 0.2 eV, P_{O_2} of the uncomplexed system rises rapidly and eventually becomes comparable to that of the complexed system.

In $Ar+O_2(0.99D_{O_2})$ at $E=1.0$ eV, the collision begins at $t_b=-0.094$ ps and ends at $t_e=+0.18$ ps; *i.e.*, the duration of collision is about 0.27 ps. The closest encounter between the collision partners occurs at $t_c=-0.016$ ps. In this collision system, the dissociation of O_2 always occurs during the recession of the collision partners; *i.e.*, the dissociation occurs after the impact at $t=t_c$. In fact, all O_2 dissociations at this collision energy occurs after the incident atom has receded from the interaction ranges ($t>t_c$). As the collision energy decreases, some dissociations occur in the time interval $t_c<t<t_e$, but the majority of dissociations occur after the collision. However, in $Ar+Ar\cdots O_2$ $(0.99D_{O_2})$, O_2 dissociation can occur either before or after the impact depending on the initial phases δ_L and δ_{O_2}. In the former case, dissociation occurs almost always during the approach of the collision partners towards each other ($t<t_b$). This is a collisionless process and it is unique to the system involving a weakly bound complex. This collisionless event is a result of intramolecular energy flow between the O_2 and weak vdW bonds through intramolecular potential coupling; see Eq. (2). In this complexed system at $E=1.0$ eV, $t_b=-0.20$ ps, $t_c=-0.081$

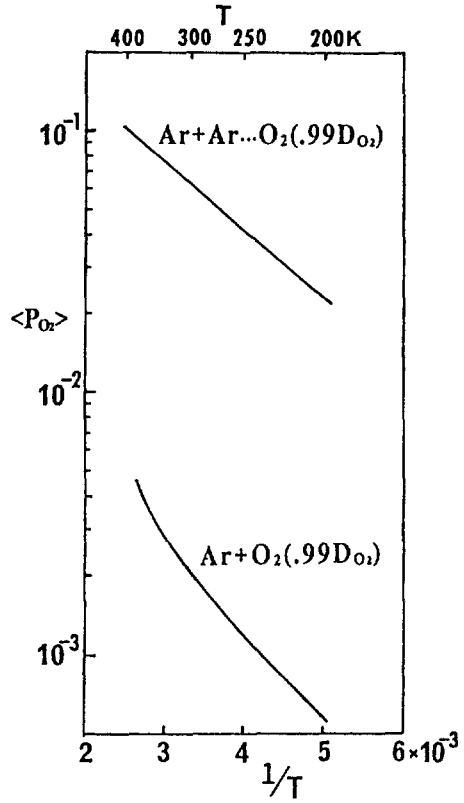

Figure 5. Semilogarithmic plot of $<P_{O_2}>$ *vs.* $1/T$ for $Ar+Ar\cdots O_2$ $(0.99D_{O_2})$ and $Ar+O_2$ $(0.99D_{O_2})$.

ps and $t_f = +0.052$ ps. Therefore, the duration of collision is 0.25 ps, which is somewhat shorter than that of the uncomplexed system, but it is now shifted to a much earlier time range. In Figure 4, we show the distribution of dissociative trajectories as a function of time for the complexed system at $E = 1.0$ eV; plotted are 156 dissociative trajectories out of 360 samples and the phase-averaged collision trajectory $x(t)$ on the same time scale. As indicated in the figure, essentially all of the pre-impact dissociations are collisionless dissociations and take place before t_b. We have started the intergration at $t^\circ = -0.59$ ps, so the first sign of collisionless dissociation appears 0.39 ps after t°. This time elapse is about twice the vibrational period of the excited molecular unit. In Figure 4, the probability of pre-impact dissociation is represented by $P_{O_2}{}^*$. This probability is very close to 0.4 over the entire collision energy range, and a diviation from this constant value is due to the statistical uncertainty, which is about 2% with 720 trajectories. The difference between P_{O_2} and $P_{O_2}{}^*$, which is represented by $P_{O_2}{}^{**}$ in Figure 3 and which determines the dissociation of O_2 after the impact, is essentially a linear function of the collision energy. It is important to note that all these post-impact dissociations occur long after the end of collision; *i.e.*, at $t > t_f$. The excited bond can even survive nearly 1.2 ps after the complex is prepared (or nearly 0.8 ps after the start of collision) before it dissociates; see the three trajectories near $t = +0.6$ ps in Figure 4. Note that during this residence time the excited O_2 in the complex undergoes about six vibrations. It should be mentioned that the weak vdW bond dissociates for all trajectories; dissociation occurs either before or after the impacts as in the case of O_2 dissociation.

The temperature dependent probability of O_2 dissociation can be defined as $<P_{O_2}> = (kT)^{-1}\int_0^\infty P_{O_2} e^{-E/kT} dE$. At 200, 300 and 400 K, the values of $<P_{O_2}>$ for $Ar+Ar\cdots O_2$ $(0.99D_{O_2})$ are 0.023, 0.062 and 0.10, respectively; see Figure 5. These values are nearly two orders of magnitude larger than those for the uncomplexed system; the corresponding values for the latter system are only 5.9×10^{-4}, 2.1×10^{-3}, and 4.4×10^{-3}. In the complexed system, since P_{O_2} increases monotonously with E, the temperature dependence is essentially determined by the Boltzmann factor, so the plot of $\ln<P_{O_2}>$ *vs.* $1/T$ leads to a straight line; *i.e.*, an Arrhenius type. The activation energy determined from the slope is 0.051 eV, which is essentially identical to the minimum energy required for the molecular unit O_2 $(0.99D_{O_2})$ to dissociate. However, in $Ar+O_2$ $(0.99D_{O_2})$, a sharp increase of P_{O_2} causes $<P_{O_2}>$ to rise more rapidly at higher temperatures thus leading to a deviation from the linear relation. As shown in Figure 3, the dissociation probability is very small at lower collision energies, where the Boltzmann factor is large, so the contribution to the integrand comming from this energy range is small

Concluding Comments

Classical trajectory calculations were carried out to examine the influence of a van der Waals bond on the dissociation of a highly excited chemical bond. Such an excited bond undergoes a large-amplitude vibrational motion with the frequency much lower than the fundamental. While the dissociation probability of O_2 in $Ar+O_2$ is comparable to that of the complexed system at higher collision energies, it is much smaller than that in the latter system in the lower collision energy range 0.05-0.2 eV. In the atom+complex collision, energy first efficiently transfers to the $Ar\cdots O_2$ bond from the incident atom and then the bond pumps the energy into the O_2 bond. Since the highly excited O_2 bond oscillates with a very low frequency, the coupling between this weakened bond and the vdW bond is sufficient enough to cause an efficient intramolecular energy flow. At lower collision energies, where the duration of collision is long, the internal energy has sufficient time to redistribute between the vdW and chemical bonds. Such an energy flow process is absent in $Ar+O_2$. As the collision energy increases, the duration of collision becomes shorter and the vdW bond dissociates before the collision. At such collision energies dissociation probabilities of both the complexed and uncomplexed systems become close to each other. An efficient intramolecular energy flow between the vdW and highly excited O_2 bonds in $Ar+Ar\cdots O_2$ causes its thermal-averaged dissociation probability to be two orders of magnitude larger than that for the uncomplexed system.

Acknowledgment. This research was supported by NSF Advanced Computing Resources granst (CHE-890039P) at the Pittsburgh Supercomputing Center. One of us (YHK) wishes to thank the Korea Science and Engineering Foundation for financial assistance.

References

1. H. K. Shin, *J. Chem. Phys.*, **87**, 993 (1987).

2. H. K. Shin, *J. Chem. Phys.*, **91**, 929 (1989).
3. H. K. Shin, *J. Chem. Phys.*, **94**, 598 (1990).
4. H. K. Shin, *J. Chem. Phys.*, **92**, 5223 (1990).
5. V. Lopez and R. A. Marcus, *Chem. Phys. Lett.*, **93**, 232 (1982).
6. R. A. Marcus, *Faraday Discuss. Chem. Soc.*, **75**, 103 (1983)
7. P. J. Rogers, J. I. Selco, and F. S. Rowland, *Chem. Phys. Lett.*, **98**, 363 (1983).
8. F. S. Rowland, *Faraday Discuss. Chem. Soc.*, **75**, 158 (1983).
9. S. P. Wrigley and B. S. Rabinovitch, *Chem. Phys. Lett.*, **98**, 363 (1983).
10. S. P. Wrigley, D. A. Oswald, and B. S. Rabinovitch, *Chem. Phys. Lett.*, **104**, 52 (1984).
11. K. N. Swamy and W. L. Hase, *J. Chem. Phys.*, **82**, 123 (1985).
12. V. Lopez, V. Fairen, S. M. Lederman, and R. A. Marcus, *J. Chem. Phys.*, **84**, 5494 (1986).
13. C. Eaborn, K. L. Jones, J. D. Smith, and K. Tavakkoli, *Chem. Commun.*, 1201 (1989).
14. T. Uzer and J. T. Hynes, *J. Phys. Chem.*, **90**, 3524 (1986).
15. H. K. Shin, *Chem. Phys. Lett.*, **156**, 536 (1989).
16. G. Henderson and G. E. Ewing, *J. Chem. Phys.*, **59**, 2280 (1973).
17. J. A. Beswick and J. Jortner, *Adv. Chem. Phys.*, **47**, 363 (1981).
18. P. Villarreal, A. Varade, and G. Delgado-Barrio, *J. Chem. Phys.*, **90**, 2684 (1989).
19. J. M. Farrar and Y. T. Lee, *Chem. Phys. Lett.*, **26**, 428 (1974).
20. J. O. Hirschfelder, C. F. Curtiss, and R. B. Bird, *Molecular Theory of Gases and Liquids*; John Wiley, New York, p. 33 (1964).
21. J. M. Huston, *Ann. Rev. Phys. Chem.*, **41**, 1 (1990).
22. J. T. Yardley, *Introduction to Molecular Energy Transfer;* Academic; New York, 1980; Chapter 4.
23. *MATH/LIBRARY;* IMSL; Houston, 1989; p. 640.
24. Reference 23, p. 1113.
25. G. Herzberg, *Spectra of Diatomic Molecules*; Van Nostrand; Princeton, 1969; Table 39.
26. J. B. Calvert and R. C. Amme, *J. Chem. Phys.*, **45**, 4710 (1966).
27. Y. Tanaka and K. Yoshino, *J. Chem. Phys.*, **53**, 2012 (1970).
28. H. K. Shin, *J. Chem. Phys.*, **79**, 4285 (1983).
29. Y. H. Kim, T. Ree, and H. K. Shin, *Chem. Phys. Lett.*, **174**, 494 (1990).

On the Critical Scattering Phenomena of a Nonpolar Binary Liquid Mixture

Dong J. Lee and Shoon K. Kim†

Department of Chemistry, National Fisheries University of Pusan, Pusan 608-023
†Department of Chemistry, Temple University, Philadelphia, PA. 19122, U.S.A. *Received March 18, 1991*

Light scattering phenomena are discussed for a nonpolar binary liquid mixture composed of an optically active solute and an optically nonactive solvent in the critical region, using the Fisher theory. Comparing them with those in the case that the Ornstein-Zernike theory is satisfied, the appropriate analytic results are obtained and discussed.

Introduction

In 1987 we[1] have proposed a general theory of multiple scattering for a nonpolar fluid composed of chiral molecules. It is based on a general theory[2] of the dielectric tensor well suited, to study the dielectric behavior in the critical region. The theory of multiple scattering has been treated as the same way as that of single scattering in the phenomenological theory given by Einstein.[3,4] The scattering intensity has been expressed in terms of the correlation function, which gives the information about the effect of fluctuations of the dielectric tensor in the sample fluid and nature of the incident light. The dielectric tensor fluctuates due to the fluctuations in density and other thermodynamic variables. We have considered the scattering only due to the density fluctuations, which plays the most dominant role in the critical region. In the subsequent paper[5] we have for the first time, discussed the effect of the double scattering on the circular intensity differences in the critical region, where the Ornstein-Zernike theory holds.

The theory of the circular intensity differences has been extended a binary liquid mixture composed of an optically active solute and an optically nonactive solvent.[6] The mixture is more suitable for experimental verification than the pure fluid. The basic difference with the latter is that there is one more extra variable in the mixture, *i.e.*, the concentration fluctuations. In fact, the concentration fluctuations play the central role in the critical region of a binary liquid mixture.[7]

The purpose of this paper is to analyze the light scattering in the critical region, where the Ornstein-Zernike theory does not hold. The correlation function of concentration fluctuations to be used is the Fisher theory of correlation function.[8,9]

At first, a general formula for the single scattering intensity and the most dominant part of the double scattering intensity are given.[6] Then, with the aid of the Fisher theory we obtain the sums and differences of components of the single and double scattering intensities approximately and discuss the circular intensity differences.